Pesticide Biochemistry and Physiology 99 (2011) 86–95

Contents lists available at ScienceDirect

Pesticide Biochemistry and Physiology

journal homepage: www.elsevier.com/locate/pest

Probing mode of action in plant cell cycle by the herbicide endothall, a protein phosphatase inhibitor

Stefan Tresch *, Jennifer Schmotz, Klaus Grossmann

BASF SE, Agricultural Research Centre, D-67117 Limburgerhof, Germany

ARTICLE INFO

Article history:
Received 18 August 2010
Accepted 9 November 2010
Available online 20 November 2010

Keywords:
BY-2 cells
Cell proliferation
Cantharidin
Endothall
Microtubules
Mitosis
Mode of action
Okadaic acid
Protein phosphatase inhibitor
S-phase detection

ABSTRACT

The mode of action of endothall, an herbicide which was reported to inhibit plant protein phosphatases 1 (PP1) and 2A (PP2A), was investigated. For initial characterization, a series of bioassays was used for comprehensive physiological profiling of endothall effects which suggested a phytotoxic mode of action similar to mitotic disrupter herbicides. Unlike known microtubule disrupters, endothall did not inhibit soybean tubulin polymerization *in vitro*. As shown in meristematic corn root tips, endothall distorted the orientation of cell division plane and microtubule spindle structures which led to cell cycle arrest in prometaphase. In tobacco BY-2 cells, malformed spindles together with prometaphase arrest of nuclei and abnormal perinuclear microtubule patterns were detected as early as 4 h of endothall treatment. These effects were also observed after treatment with other protein phosphatase inhibitors, cantharidin and okadaic acid, which phenocopied the mitotic changes described in *tonneau1* (*ton1*) and *tonneau2* (*ton2*) *Arabidopsis* mutants. These mutants are defective in TONNEAU2 (TON2) protein, a regulatory subunit of PP2A, which governs cell division plane and microtubule orientation. Therefore, PP2A/TON2 phosphatase complex is suggested to be an *in planta* molecular target of endothall. However, in BY-2 cells, additional effects of endothall, including inhibition of S-phase initiation and DNA synthesis, detected by 5-ethynyl-2′-deoxyuridine (EdU) incorporation, and condensed nuclei arrested in late mitosis were observed which were not reported in *Arabidopsis ton1* and *ton2* mutants. This result indicates that two additional checkpoints in cell cycle were blocked by endothall which are probably not associated with TON2-pathway inhibition. Possibly, inhibition of PP1 and/or other PP2A protein phosphatases are involved in the regulation of these cell cycle phenomena.

1. Introduction

The herbicidal properties of endothall (7-oxabicyclo[2.2.1]heptane-2,3-dicarboxylic acid) were first reported by Tischler et al. in 1951 [1]. The compound was commercially introduced by Sharples Chemical Corporation (now Cerexagri Inc.) for selective, postemergence control of several annual broadleaf and grass weeds in sugar beets [2]. Additionally, it can be applied as a preharvest desiccant in potatoes, alfalfa and clover seed crops [2]. Endothall is also used to control algae and several other aquatic weeds [2].

Early reports described cytological studies in cells of *Pisum sativum* which show effects of endothall on chromosome distribution within mitosis [3]. These effects of endothall, which included chromosome loss during metaphase, the presence of few micronuclei structures, and the absence of prometaphase, could be distinguished from other microtubule assembly inhibitors such as colchicine [3]. In other plant systems, endothall, applied at high concentrations, was found to increase leakage of electrolytes followed by tissue necrosis which suggested membranes as an early site of endothall injury [4]. Interference with plant lipid biosynthesis [5] and RNA and protein synthesis was also reported [6–8]. As a more specific effect, endothall and the structurally related cantharidin have been shown to inhibit mammalian protein phosphatase 1 (PP1) and protein phosphatase 2A activity (PP2A) *in vivo* [9,10]. Cantharidin is known as the toxic ingredient of a variety of blister beetles and was found to bind to mammalian PP2A [9,11]. Moreover, Li et al. [11] and Ayaydin et al. [12] have demonstrated that endothall and cantharidin also inhibit plant PP1 and more sensitive PP2A activity in cultured alfalfa cells and intact spinach leaves. In the latter tissue, inhibition of PP2A activity was accompanied by decreased light-induced activation of nitrate reductase [11]. However, the exact herbicidal mechanism and mode of action of endothall is not yet clarified.

Abbreviations: EdU, 5-ethynyl-2′-deoxyuridine; MI, mitotic index; MSTB, microtubule stabilizing buffer; PI, proliferation index; PP1, protein phosphatase 1; PP2A, protein phosphatase 2A; TBS, tris buffered saline.

* Corresponding author. Address: Speyerer Str. 2, D-67117 Limburgerhof, Germany. Fax: +49 621 6027176.

E-mail address: stefan.tresch@basf.com (S. Tresch).

0048-3575/$ - see front matter © 2010 Elsevier Inc. All rights reserved.
doi:10.1016/j.pestbp.2010.11.004

In order to study a possible causality between the known inhibition of protein phosphatases and processes leading to plant damage, we analyze the herbicidal mode of action of endothall in more detail. For initial characterization, an array of bioassays was used in a physionomics approach for comprehensive physiological profiling of endothall effects [13]. Cantharidin and the mitotic disrupter herbicide pendimethalin were included in this investigation. Since similarities to pendimethalin and cantharidin were observed, the effects of endothall on cell division processes were studied in corn root tips and tobacco BY-2 suspension cells in comparison to cantharidin and the known protein phosphatase inhibitor okadaic acid. Here, cytological and biochemical methods were used which include immunocytochemical fluorescence techniques and *in vitro* polymerization of plant tubulin. This is the first time detailed analysis of endothall effects has been done in plant tissue. The results suggest that effects of endothall on microtubule cytoskeleton arrangement and mitotic structures, possibly mediated by protein phosphatase inhibition, mainly contribute to the herbicidal mode of action.

2. Materials and methods

2.1. Chemicals

Endothall (7-oxabicyclo[2.2.1]heptane-2,3-dicarboxylic acid, CAS No. 62059-43-2), cantharidin (2,3-dimethyl-7-oxabicyclo[2.2.1] heptane-2,3-dicarboxylic anhydride, CAS No, 56-25-7) and okadaic acid (CAS No. 78111-17-8) were obtained from Sigma–Aldrich, Deisenhofen, Germany.

2.2. Bioassays

The bioassays of the physionomics approach were carried out as described elsewhere [13]. In the heterotrophic cell suspension assay, freely suspended callus cells from *Zea mays* L. (DSM Collection of Plant Cell Cultures, Braunschweig, Germany) were cultivated in a modified Murashige-Skoog medium as described previously [13]. The cells were subcultured at 7-day intervals. Acetone solutions of the compounds were pipetted into plastic tubes, and the solvent was allowed to evaporate before adding 2 ml of exponentially growing cell suspensions. The tubes (three replicates) were shaken at 300 rpm and 25 °C in the dark on a rotary shaker. After incubation for 8 days, the conductivity of the medium was measured as the parameter for cell division growth [13].

For the algae bioassay, cells of *Scenedesmus obliquus* Kützing 276-3a (Culture Collection Göttingen, Göttingen, Germany) were propagated photoautotrophically [13]. The bioassay was carried out in plastic microtitre dishes containing 24 wells. Before loading each well with 0.5 ml cell suspension, 0.5 ml medium and compound in acetone solution were added, allowing sufficient time for the organic solvent to volatilize. The 15 additional compartments between the wells were filled with sodium carbonate/bicarbonate buffer. The dishes were sealed with plastic lids and incubated on a shaker under continuous light with 60 $\mu mol\ m^{-2}\ s^{-1}$ photon irradiance at 23 °C. After 24 h, cell density was measured photometrically.

For the *Lemna* bioassay, stock cultures of *Lemna paucicostata* (L.) Hegelm. (collection Prof. R Kandeler, University of Vienna, Austria) were propagated mixotrophically in an inorganic medium containing sucrose [13]. The bioassay was conducted under aseptic conditions in plastic petri dishes (5 cm diameter) which contained 15 ml medium without sucrose. The test compounds were added to the dishes in acetone solution, and the organic solvent was allowed to volatize before loading them with four fronds each. The culture dishes were then closed with plastic lids and incubated under continuous light (Philips TL white fluorescent tubes, 40 $\mu mol\ m^{-2}\ s^{-1}$ photon irradiance, 400–700 nm) in a growth chamber at 25 °C. Eight days after treatment, the increase in the area covered by the fronds in each dish was determined as the growth parameter using an image analyzing system (LemnaTec Scanalyzer; LemnaTec, Würselen, Germany).

For the isolated shoot bioassay, seedlings of mustard (*Sinapis alba* L.) were grown under standardized greenhouse conditions. The shoots were removed, weighted and placed upright in plastic vials (25 mm diameter, 38 mm height; Greiner, Nürtingen, Germany) which contained 12 ml double-distilled water and the test compound added in acetone solution (1 $ml\ l^{-1}$ final concentration of Aceton) [13]. To avoid evaporation, the vials were closed with plastic covers with slits into which the shoots were fitted (three shoots per vial). The vials were cultivated in growth chambers with a 16:8 h light:dark photoperiod at 21 °C and 75% relative humidity (light: Osram krypton 100 W lamps and Osram universal white fluorescent tubes, 200 $\mu mol\ m^{-2}\ s^{-1}$ photon irradiance, 400–700 nm). After 3 days, changes in fresh weight were measured by weighing the shoots and subtracting the values from initial weights.

To determine effects on the Hill reaction, thylakoids were isolated from shoots of young plants of *Triticum aestivum* L., and assay was performed as previously described [13]. Isolated thylakoids were suspended in a reaction medium (0.75 ml) that contained sucrose 0.1 M, tricine–NaOH (pH 8.0) and 50 mM, magnesium chloride 5 mM and chlorophyll 41 $\mu g\ ml^{-1}$. The assay mixture included thylakoid suspension (0.23 ml), test compound dissolved in acetone + water (80 + 20 by volume; 0.05 ml) and ferricyanide (5 mM; 0.02 ml). During the subsequent illumination for 4 min with 1300 $\mu mol\ m^{-2}\ s^{-1}$ photon irradiance, ferrocyanide was formed in the Hill reaction. Then, in the darkness, the ferrocyanide was allowed to react with ferric salt to form the ferrous salt, which produced a complex with phenanthroline. The complex was measured photometrically at 510 nm.

For the germination bioassay, seed of cress (*Lepidum sativum* L.) were placed in glass petri dishes (5 cm in diameter) filled with vermiculite substrate. Stock solutions of the test compounds in acetone were added together with 12 ml water (1 $ml\ l^{-1}$ final concentration of aceton) [13]. Control seeds were moistened only with water and acetone. The dishes were incubated in a growth chamber at 25 °C in the dark for 3 days. Inhibition of germination and seedling development was evaluated visually (0 = no influence, 100 = total inhibition). Afterwards, the dishes were incubated for a further 3 days under light conditions (16:8 h light:dark at 25 °C and 75% relative humidity, 230 $\mu mol\ m^{-2}\ s^{-1}$ photon irradiance, 400–700 nm), and seedling development and plant symptoms were evaluated.

To determine carbon dioxide uptake as a parameter for carbon dioxide assimilation, plants of *Galium aparine* L. that had been raised under controlled conditions to the second whorl stage were cultivated hydroponically in illuminated glass chambers (four plants per chamber, three replications) which received a constant stream of air [13] After foliar treatment with the compound, the amount of carbon dioxide assimilated per unit time was determined continuously for 24 h from the difference between the carbon dioxide contents of the inflowing and outflowing air streams.

For the determination of respiration, 18 ml cell suspensions of *Galium mollugo* L. (DSM Collection of Plant Cell Cultures, Braunschweig, Germany) were treated with compound in plastic vessels for 5 h in the dark on a rotary shaker (1 $ml\ l^{-1}$ final concentration of aceton). Samples of 5 ml cell suspension were then transferred to plastic tubes for measurement of oxygen consumption using the dissolved oxygen measuring system inoLab Oxi Level 3 with the oxygen sensor CellOx 325 (WTW, Weilheim, Germany). Respiration inhibition was measured as oxygen consumption in $\mu l\ l^{-1}$ per min in comparison to control. [13].

To determine the uncoupler activity of compounds, *Lemna* plants were pretreated with the mitochondrial potential sensor dye JC-1 (10 μg ml^{-1} in nutrient solution; Invitrogen Ltd., Paisley, United Kingdom) for 30 min. JC-1 exhibits potential-dependent accumulation in mitochondria, indicated by a fluorescence emission shift from green to red [13]. Mitochondrial membrane depolarization is indicated by a decrease in the red/green fluorescence intensity ratio. After staining, *Lemna* plants were washed and loaded into 48 well plastic microtitre dishes, with each well containing four fronds, 0.5 ml medium and compound added in acetone solution (1 ml l^{-1} final concentration of aceton). After treatment for 90 min, *Lemna* plants were transferred to slides for fluorescence microscopic observation of root mitochondria using an Olympus BX61 epifluorescence microscope (Hamburg, Germany).

The results were expressed as percentage inhibition. Mean values of three replicates are given as the percentage inhibition relative to control. Individual standard errors were less than 10%. All experiments were repeated at least twice and proved to be reproducible. The results of representative experiments are shown.

2.3. Histochemical determinations

Histochemical studies were performed according to [14]. Uniformly germinated seedlings of *Z. mays* cv. Amadeo with a root length of 3 cm were transferred into 50 ml glass vessels (one seedling per vessel, three replications) in half strength Linsmaier–Skoog [15] nutrient solution (16:8 h light:dark at 25 °C and 75% relative humidity, 250 μmol m^{-2} s^{-1} photon irradiance, 400–700 nm; fluorescent lamps, radium HRLV). After 4 h of adaption compound was added to the medium in dimethyl sulfoxide (DMSO) solution (1 ml l^{-1} final concentration of DMSO). Controls received a corresponding quantity of DMSO alone, with no adverse effect on seedling growth.

After 4 or 24 h treatment, primary root tips of 5 mm length with meristematic and elongation zones were harvested, fixed in 37 g l^{-1} paraformaldehyde in phosphate buffered saline (PBS, pH 7.4), and embedded in paraffin as described elsewhere [16]. For observation of nuclear DNA longitudinal sections of 7 μm thickness were obtained with a rotary microtome (Leica RM 2165; Leica, Wetzlar, Germany) and placed on Polysine™ slides (Menzel, Braunschweig, Germany). After deparaffinazing according to standard methods [16], nuclear DNA was stained with Hoechst 33342 (0.75 μg ml^{-1} in phosphate buffered saline, pH 7.5; Invitrogen Ltd.) for 5 min. To avoid fast fluorescence quenching, the stained slides were mounted with ProLong® Antifade (Invitrogen Ltd.).

Microtubules or tubulin were labeled with monoclonal antibodies against polymerized β-tubulin (Sternberger Monoclonals, Lutherville, MD, USA). The primary antibodies were marked with fluorescent Alexa Fluor® 488-conjugated secondary antibodies (Invitrogen), as previously described [14]. Firstly, root tips were fixed in 40 g l^{-1} paraformaldehyde in microtubule-stabilizing buffer (MSTB, pH 6.9) which contained 60 mM PIPES (piperazine-*N*, *N*′-bis(2-ethanesulfonic acid)), 25 mM HEPES (*N*-2-hydroxyethylpiperazine-*N*′-2-ethanesulfonic acid), 10 mM EGTA (ethylenedioxy-bis(ethylenenitrilo)tetraacetic acid) and 0.2 g l^{-1} $MgSO_4 \cdot 6H_2O$ for 14 h. Root tips were than subjected to a sequential series of sucrose infiltration, which contained 120, 140 and 160 g l^{-1} sucrose in MSTB buffer, for 1 h each step. Afterwards, they were frozen in liquid nitrogen. Longitudinal sections of 15 μm thickness were obtained with a cryostat (Frigocut-2800 E; Reichert-Jung, Leica) and placed on Polysine™ slides. The slides were incubated with DAKO antibody diluent (DAKO GmbH, Hamburg, Germany) for 20 min to block unspecific binding sites. Incubation with tubulin antibodies and secondary antibodies was carried out for 30 min. The primary and secondary antibodies were diluted with DAKO antibody diluent to 1:200 and 1:100, respectively. After staining of nuclear DNA with Hoechst 33342 (0.75 μg ml^{-1} in phosphate buffered saline, pH 7.5) for 5 min, labeled slides were mounted with ProLong® Antifade (Invitrogen) for microscopic observation.

Microscopic observations were carried out using an Olympus BX61 epifluorescence microscope with standard bandpass filter sets (Hamburg, Germany) and a confocal laser scanning microscope (Leica DMRXA TCS SP2) equipped with UV and krypton-argon laser.

2.4. Cytological investigations of BY-2 cells

For determination of distribution of mitotic phases, visualization of S-phase activity and observation of microtubules in cell culture, freely suspended cells of *Nicotiana tabacum* L., BY-2 cultures [17] were used. The cells were subcultured in Linsmaier and Skoog nutrient solution (including 3% sucrose, w/v, 1 μM 2,4-dichlorophenoxyacetic acid; [15]) at 7-day intervals and agitated on a rotary shaker at 115 rpm at 25 °C in the dark. For compound treatment 2 μl DMSO solutions were pipetted into plastic tubes before adding 2 ml of 3-day old cell suspensions. Control samples where treated with 2 μl DMSO alone. The tubes were shaken at 300 rpm and 25 °C in the dark on a rotary shaker. After incubation for 4 and 24 h, cells were fixed and stained with a modified method described by [18]. The cells were sedimented for 5 min and supernatant nutrient solution was discarded. Subsequently, 1 ml fixative solution (3.7% paraformaldehyd in MSTB) was applied to cells for at least 15 min at 4 °C. Afterwards cells were washed with 1 ml 0.05 mM tris buffered saline (TBS, pH 7.6) at 4 °C for 5 min and 1 ml acetone + methanol (1 + 1 by volume) solution was added at −20 °C for 15 min. Next to a washing step with TBS, the cell wall was digested for better antibody penetration with 0.5 ml enzyme solution in TBS (5 U ml^{-1} cellulase Onozuka R-10, w/v, SERVA Electrophoresis, Heidelberg, Germany and 0.05% pectolyase, v/v; Sigma–Aldrich; in TBS) for 15 min. Then, cells were treated for 5 min with 0.5 ml TBS containing 0.05% detergent Tween 20 and subsequently 0.5 ml DAKO antibody diluent for additional 20 min. For staining, cells were treated with 0.3 ml anti-β-tubulin antibody (Clone TUB 2.1; Sigma–Aldrich) solution as 1:100 dilution in DAKO antibody diluent (DAKO GmbH) for 25 min. After washing with TBS containing 0.05% Tween 20 for 5 min, cells were treated for 30 min with secondary antibody labeled with Alexa Fluor® 488 (Invitrogen). Subsequently, nuclear DNA was stained with Hoechst 33342 (10 μg ml^{-1} in 0.05 M TBS) for 10 min. All procedures after acetone + methanol treatment were done at room temperature. Labeled cells were pipetted on glass slides and mounted with ProLong® antifade (Invitrogen) prior to microscopic observation on Olympus BX61 microscope (Hamburg, Germany).

Effects on DNA synthesis in S-phase of proliferating BY-2 cells was studied using Click-iT® technology (Invitrogen) in combination with the nucleoside analog 5-ethynyl-2′-deoxyuridine (EdU, Invitrogen) as described by [19,20]. EdU is a nucleoside analog of thymidine and is incorporated into DNA during active DNA synthesis. Detection of EdU, which contains an alkyne group, was done with reactive Alexa Fluor® 488 dye which contained an azide group. Based on the principle of click chemistry, reactive Alexa 488 dye was used to detect incorporated EdU in proliferated nuclei. EdU (10 μM) was applied simultaneously to compound treatment for 4 and 24 h as described above. Control samples were treated with EdU, compound or solvent alone. After treatment, harvested cells were fixed as described above. After acetone + methanol treatment, cells were washed with phosphate buffer and EdU staining was performed according to standard protocol of Click-iT® EdU Imaging Kit (Invitrogen) as described by supplier. Total nuclear DNA was stained with Hoechst 33342 as described. Subsequently, cells were mounted on glass slide with ProLong® antifade and observed under epifluorescence microscope BX61 (Olympus).

Mitotic index (MI) was calculated as percent of cells in mitosis related to total counted cells. For classification of the mitotic phases, Hoechst 33342 stained nuclei were assigned by microscopic observation to interphase or a distinct mitotic phase. In addition, abnormal nuclei in cells were classified as prometaphase arrested, condensed, relaxed or multinuclear. Detection of DNA synthesis in S-phase of proliferating cells was carried out in a parallel experiment. Proliferation index (PI) was calculated as percent of cells showing nuclear DNA synthesis by EdU coupled Alexa Fluor® 488 fluorescence related to total counted cells. In each study, at least 500 cells were counted in two replicate samples. All experiments were replicated at least twice and proved to be reproducible.

2.5. Tubulin polymerization assay

Determination of compound effects on tubulin polymerization *in vitro* was studied using a microassay biochemical kit from Cytoskeleton Inc. (Denver, CO, USA) with soybean tubulin according to the standard protocol (Tebu-Bio, Offenbach, Germany) as described [21]. Soybean tubulin was isolated from seedlings in greater than 90% purity. The assay utilizes 4′,6-diamidino-2-phenylindole (DAPI) as fluorescent compound which binds to formed microtubules with higher affinity than tubulin heterodimers [22]. The result is a fluorescence signal that closely follows microtubule formation. The microassay was performed in 384-well plates (three replications) at 25 °C, and fluorescence was measured every 30 s during a time of 60 min at an excitation of 360 nm and an emission wavelength of 405 nm using a temperature-controlled fluorescence plate reader (SpectraFluor Plus; Tecan Deutschland GmbH, Crailsheim, Germany) The extent of polymerization in each assay was measured as mean of arbitrary fluorescence units during plateau phase of polymerization (range from 34 to 60 min of incubation). Inhibition of tubulin polymerization by compound treatment was expressed in percentage related to maximum polymerization of control assays.

3. Results

3.1. Physiological profiling using bioassays

In initial experiments, a set of established bioassays were used to characterize and classify the mode of action of endothall in the search for its inhibitory process leading to plant damage. These systems included heterotrophic corn (*Z. mays*) and photoautotrophic green alga (*S. obliquus*) cell suspensions, duckweed (*L. paucicostata*), isolated mustard (*S. alba*) shoots and germinating cress (*L. sativum*) seeds. The test panel was completed by assays for monitoring physiological processes, including the Hill reaction of isolated wheat thylakoids, respiration by measuring oxygen consumption in heterotrophic *G. aparine* cell suspensions, membrane function and uncoupler activity determined in *Lemna* root mitochondria using the potential sensor JC-1, carbon gas-exchange measurements in cleaver (*G. aparine*) plants. The response pattern represents a fingerprint of a phytotoxic compound, which has proved to be typical of its mode of action [13].

The response pattern of endothall (Fig. 1) shows strong inhibitory effects in bioassays with growth governed by high cell division activity including heterotrophic cell suspensions, *Lemna* and germinating seeds of cress. In the latter bioassay, in darkness, hypocotyl and root growth of cress seedlings were stunted and roots were swollen. In light, growth inhibition of cress seedlings, *Lemna* and isolated mustard shoots were accompanied by necrosis of shoot tissue. Light-dependent photosynthetic Hill reaction, carbon assimilation and green algae growth were less affected. Moderate effects were found on mitochondrial membrane potential (uncoupler activity) in all concentrations tested. No effects were observed on respiratory activity as measured through oxygen consumption in heterotrophic cell suspension. In summary, typical plant symptoms elicited by endothall were growth inhibition and swelling of roots on the one hand and tissue desiccation and necrosis on the other (Fig. 1).

The response pattern of cantharidin (Fig. 1) and pendimethalin (Fig. 1) in the bioassays were quite similar to endothall (Fig. 1).

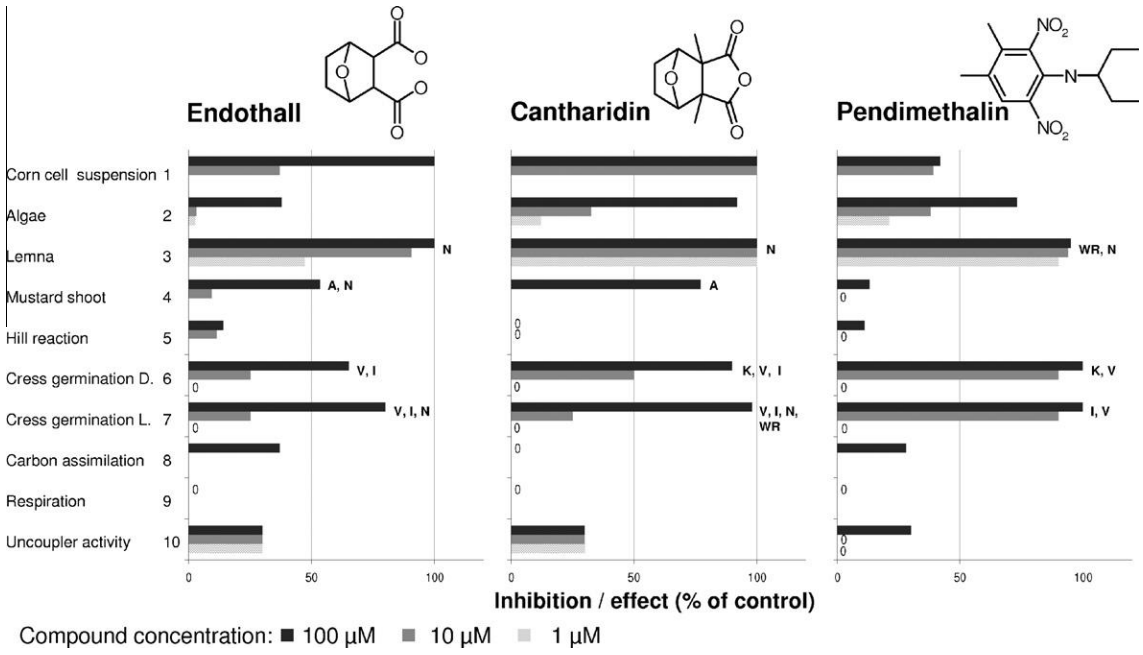

Fig. 1. Effects of endothall, cantharidin and pendimethalin in bioassays including corn and algal cell suspensions, duckweed, isolated mustard shoots, germinating cress seeds, the Hill reaction of isolated wheat thylakoids, respiration by measuring oxygen consumption in heterotrophic *Galium* cell suspensions, uncoupler activity in *Lemna* root mitochondria and carbon assimilation in *Galium* plants. SE of the mean in all cases was less than 10%. Symptoms observed: A, desiccation; I, root growth inhibition; K, reduced seed germination; N, necrosis; V, root swelling; WR, intensified green leaf pigmentation.

Particularly, root growth inhibition and swelling of root tips in dark-grown cress seedlings were typical of all compounds tested. However, the overall activity of cantharidin was higher than that of endothall. Here, cantharidin clearly shows higher activity in the algae bioassay than endothall. Different to endothall and cantharidin, the mitotic disrupter herbicide pendimethalin showed necrosis only at the meristematic leaf area in *Lemna*. In addition, slight uncoupler activity of pendimethalin was only observed at 100 μM.

3.2. Effects on tubulin polymerization in vitro

Induced root swelling into a club shape which was caused by endothall and cantharidin (Fig. 1) is very characteristic for mitotic disrupter herbicides such as pendimethalin, cyanoacrylates or flamprop-*m*-methyl [14,21,23]. Therefore, the effect of endothall on tubulin polymerization to microtubules *in vitro* was measured with purified tubulin from soybean (Table 1). It was shown for pendimethalin that tubulin polymerization was completely blocked at 50 μM and 10 μM. At 3 μM, pendimethalin inhibited polymerization by 48%, in comparison to control. In contrast, the *in vitro* polymerization of plant tubulin by endothall was minimal. At the highest concentration of 50 μM which could be tested in the assay, only 12% inhibition was measured.

3.3. Endothall influences cell division plane and mitotic spindle formation in tissue of corn root tips

To study effects on cell division processes *in vivo*, the effect of endothall on mitosis and microtubule cytoskeleton in meristematic tissue of corn root tips was analyzed (Fig. 2). Corn seedlings were treated hydroponically with 10 and 100 μM endothall for 4 and 24 h, respectively. The tips of primary and adventitious roots were sampled, and serial longitudinal sections were processed for microscopic examination. In order to investigate compound effects on mitosis and microtubules, nuclear DNA was stained with Hoechst 33342, and microtubule arrays were visualized by means of fluorescence-labeled monoclonal antibodies against β-tubulin.

After treatment with 10 μM endothall, cells with metaphase and prometaphase stages accumulated within 4 h (Fig. 2B), in comparison to control (Fig. 2A). As illustrated in Fig. 2B by arrows, endothall caused a change in the orientation of mitotic metaphase chromosomes. Most of the chromosomal metaphase plates showed a diagonal orientation and were not aligned transversally as in control tissue (Fig. 2A). Therefore, the cell division plane in endothall-treated tissue was disoriented. Prometaphase stages were also detected after endothall treatment (Fig. 2B, indicated by star). However, anaphase and telophase were not found which indicates cell cycle arrest in a condensed state of metaphase or prometaphase. Concomitantly, formation and orientation of spindle microtubule arrays were largely affected (Fig. 2D and E). Phragmoplast microtubule arrays were observed only scarcely and cortical microtubules decreased after 4 h of endothall treatment, dependent on concentration (Fig. 2D and E). Spindle microtubules were severely disorganized and unevenly oriented. Treatment with high endothall concentration (100 μM) led to a more condensed microtubule spindle array with shortened microtubule bundles, compared to control (Fig. 2E). Spindle microtubule length at 10 μM endothall treatment was not visibly changed (Fig. 2D). At both concentrations, the majority of microtubule spindle arrays were diagonally oriented and not longitudinally as in untreated cells. The arrays were unevenly arranged and apparent microtubule spindle poles showed malformations including condensed and twisted structure or widespread and disorganized appearance (Fig. 2D and E).

Table 1
Effect of endothall and pendimethalin on *in vitro* polymerization of soybean tubulin. The microassay was performed in three replications of each treatment. Inhibition of tubulin polymerization by compound treatment was expressed in percentage related to maximum polymerization in control assays.

Compound	(μM)	Inhibition of tubulin polymerization compared to control (%)
Endothall	50	12
	10	0
	3	0
Pendimethalin	50	100
	10	100
	3	48

3.4. Endothall influences mitotic spindle organization, causes unusual prometaphase arrest and reduces proliferation in BY-2 cells

To elucidate effects on mitosis and microtubule cytoskeleton in more detail, endothall was investigated in comparison to the structurally related cantharidin and the known phosphatase inhibitor okadaic acid [24] in tobacco BY-2 suspension cells, a powerful system to analyze cell cycle processes [17].

Staining of microtubules in endothall-treated BY-2 cells with monoclonal antibodies against β-tubulin (Fig. 3) showed comparable effects on spindle microtubules as observed in tissue of corn root tips (Fig. 2). Most of the spindle structures observed in endothall-treated BY-2 cells were unequally oriented and showed disoriented and multipolar spindles (Fig. 3B and J), compared to control (Fig. 3A and I). After only 4 h of treatment, microtubule spindle were asymmetrically dispersed and no longer oriented towards one spindle pole (Fig. 3B). In contrast to endothall, cells treated with cantharidin or okadaic acid showed strong accumulation of perinuclear microtubules (Fig. 3C and D). Abnormal mitotic spindle structures, similar to that observed in endothall-treated cells (Fig. 3B and J), could be found rarely in cantharidin (Fig. 3C and K) or okadaic acid (Fig. 3D and L) treated cells after 4 h (Fig. 3C and D) and 24 h (Fig. 3K and L).

In endothall-treated cells, malformed spindles ultimately led to disturbed chromosome arrangements which showed accumulation of prometaphase nuclei in mitosis as early as 4 h after treatment (Fig. 3F and N). Disturbed chromosome arrangement between prophase and metaphase is the dominant visual effect of endothall within 4 h of treatment (Fig. 4). The structure of arrested prometaphase were similar to abnormal, arched metaphases with single chromosomes outside the metaphase plane (Fig. 3F). This phenomenon is different to prometaphase arrest elicited by other mitotic disrupter herbicides, such as pendimethalin (Fig. 4) or cyanoacrylates (not shown), which induce prometaphase arrest by microtubule assembly inhibition and disrupting microtubule stability [14,25] Similar to endothall effects on mitotic nuclei, cantharidin and okadaic acid caused accumulation of prometaphase nuclei (Fig. 4). Additionally, strongly condensed nuclei, characterized by their compact and homogenous Hoechst 33342 stain, were observed particularly after treatment with the protein phosphatase inhibitors okadaic acid, cantharidin and endothall but not after treatment with the microtubule assembly inhibitor pendimethalin (Fig. 4). Strongest accumulations of condensed nuclei were elicited by okadaic acid and cantharidin treatment (Figs. 3G and H, 4 and 5). Both compounds also caused strong accumulations of nuclei with relaxed DNA structures (Figs. 3G, H and 5), whereas endothall was less effective (Fig. 5). In contrast, pendimethalin showed only accumulated prometaphase nuclei and cells with multinuclei, whereas cells with condensed nuclei or relaxed nuclei did not occur (Fig. 5).

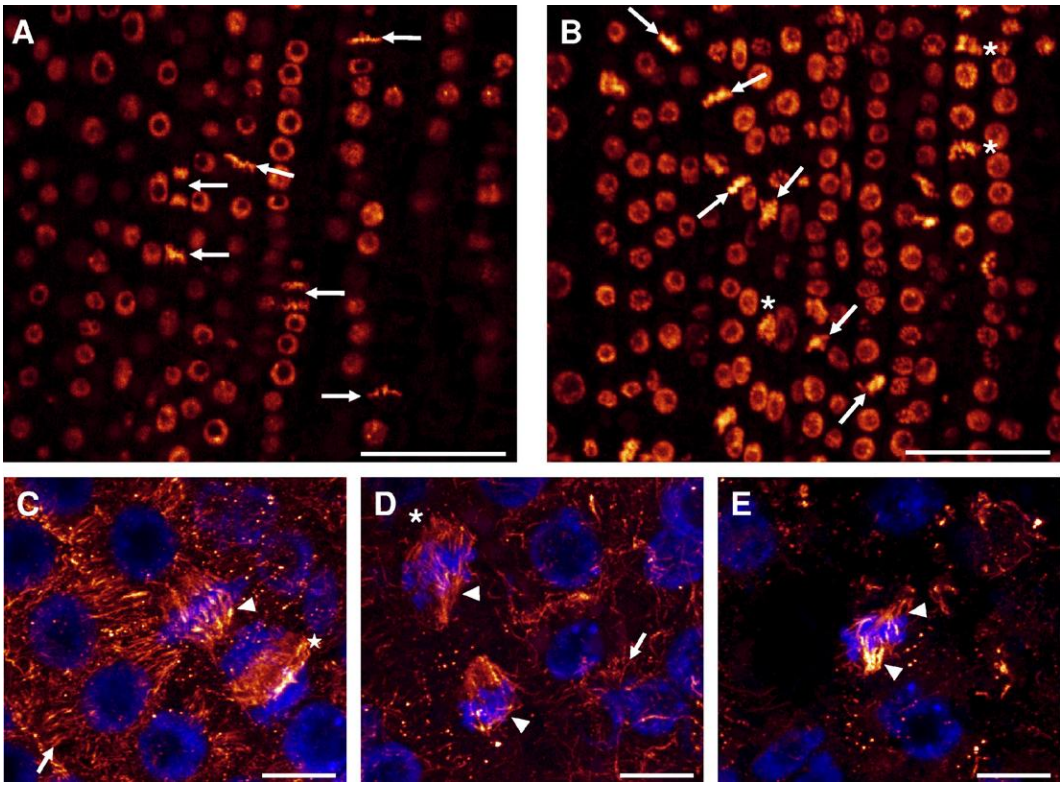

Fig. 2. Effects of endothall on orientation of division plane, mitosis and microtubule cytoskeleton in meristematic corn root cells. Seedlings were treated with 10 and 100 μM endothall for 4 h hydroponically. Tips of primary and adventitious roots were sampled, and serial longitudinal sections were processed for microscopic observation. (A) Control root tips and (B) 10 μM endothall treatment: Hoechst 33342 staining of mitotic structures. The orientation of the cell rows in the images is exactly longitudinal. The lower part of the images corresponds to the apical part of the root. Transversal (A) or diagonal (B) orientation of the division plane is denoted by arrow direction. Control cells (A) undergoing mitosis; metaphase and telophase stages (arrows) are shown. Endothall treated cells (B) showing disoriented metaphase stages (arrows) and malformed prometaphase stages (star). (C) Control cells, (D) 10 μM endothall, (E) 100 μM endothall treated cells: immunofluorescent staining of microtubules using monoclonal antibody against tubulin (red). Nuclear DNA was stained with Hoechst 33342 (blue). Control cells (C) show cortical (arrow), spindle (arrowhead) and phragmoplast microtubules (star). Endothall treated cells (10 μM) (D) show disorganized, uneven spindle (arrowhead) with spread microtubule spindle pole zone (star) and reduced cortical microtubules (arrow). Endothall treated cells (100 μM) (E) show accumulation of disorganized microtubule spindle and twisted or uneven spindle apparatus (arrowhead). Bar: 50 μm (A and B); 10 μm (C and D and E).

To determine if either the cells enter the S-phase or the cell cycle was blocked at G1/S transition by the compounds, cell proliferation rate was analyzed. DNA synthesis in proliferating cells was detected using a method based on the incorporation of the artificial nucleotide 5-ethynyl-2′-deoxyuridine (EdU) and its subsequent detection by a fluorescent azide, as described by [19]. BY-2 cells undergoing S-phase incorporate EdU into DNA during replication which results in a fluorescent signal after staining procedure (Fig. 3M–P). Proliferation index (PI) was determined as percent of fluorescent cells to total counted cells. As shown in Table 2, endothall decreased PI moderately after 4 h and strongly after 24 h of treatment in a dose dependent manner, respectively. Compared to endothall, cantharidin and okadaic acid caused a strong decrease of PI even at lower compound concentrations. No effect was observed by pendimethalin. A more detailed analysis of mitotic DNA stages after cantharidin and okadaic acid treatment revealed condensed nuclei which did not show DNA synthesis during 24 h of treatment (Fig. 3O and P). This effect was similar in endothall-treated cells. But different to cantharidin and okadaic acid, endothall additionally induced prometaphase nuclei which showed fluorescent staining for S-phase transition. Consequently, these cells were still able to enter G2/M transition during time of treatment (Fig. 3N). Accumulation of condensed nuclei without DNA synthesis in cantharidin, okadaic acid and endothall-treated cells clearly shows that nuclei, classified as condensed nuclei, did not undergo S-phase.

Shown as percent of affected nuclei in cell cycle to total counted cells (Fig. 5), the overall effect of endothall at 100 μM (15%) is lower compared to 10 μM cantharidin (34%), 10 μM okadaic acid (19%) or 10 μM of the microtubule assembly inhibitor pendimethalin (59%) after 24 h of treatment. Mitotic index (MI) as percent of cells in mitosis to total counted cells (Table 2) was only slightly changed 4 h after treatment with endothall, cantharidin and okadaic acid. In contrast, 10 μM pendimethalin increased MI from nearly 10% in control to 18% in treated cells (Table 2). After 24 h of treatment, endothall, cantharidin and okadaic acid mostly decreased MI, whereas pendimethalin showed an increase in MI from nearly 15% in control to 23% in treated cells (Table 2).

4. Discussion

The herbicide endothall was presented for the first time in 1951 [1]. However in spite of extensive research, the herbicide mode of action has not been clarified. The molecular interactions of endothall and the structurally related cantharidin with serine/threonine-specific plant protein phosphatases PP1 and PP2A have been shown and related to inhibitory effects on nitrate assimilation [11] and cell cycle processes [3,12].

To characterize the mode of action of endothall and the inhibitory process leading to plant damage, we used a set of bioassays for comprehensive physiological profiling of endothall and cantharidin effects. The results can be interpreted directly, or a library of response patterns of compounds with known modes of action can be screened for similarities to provide some clues that can be used as an aid to direct further investigations [13]. The overall response

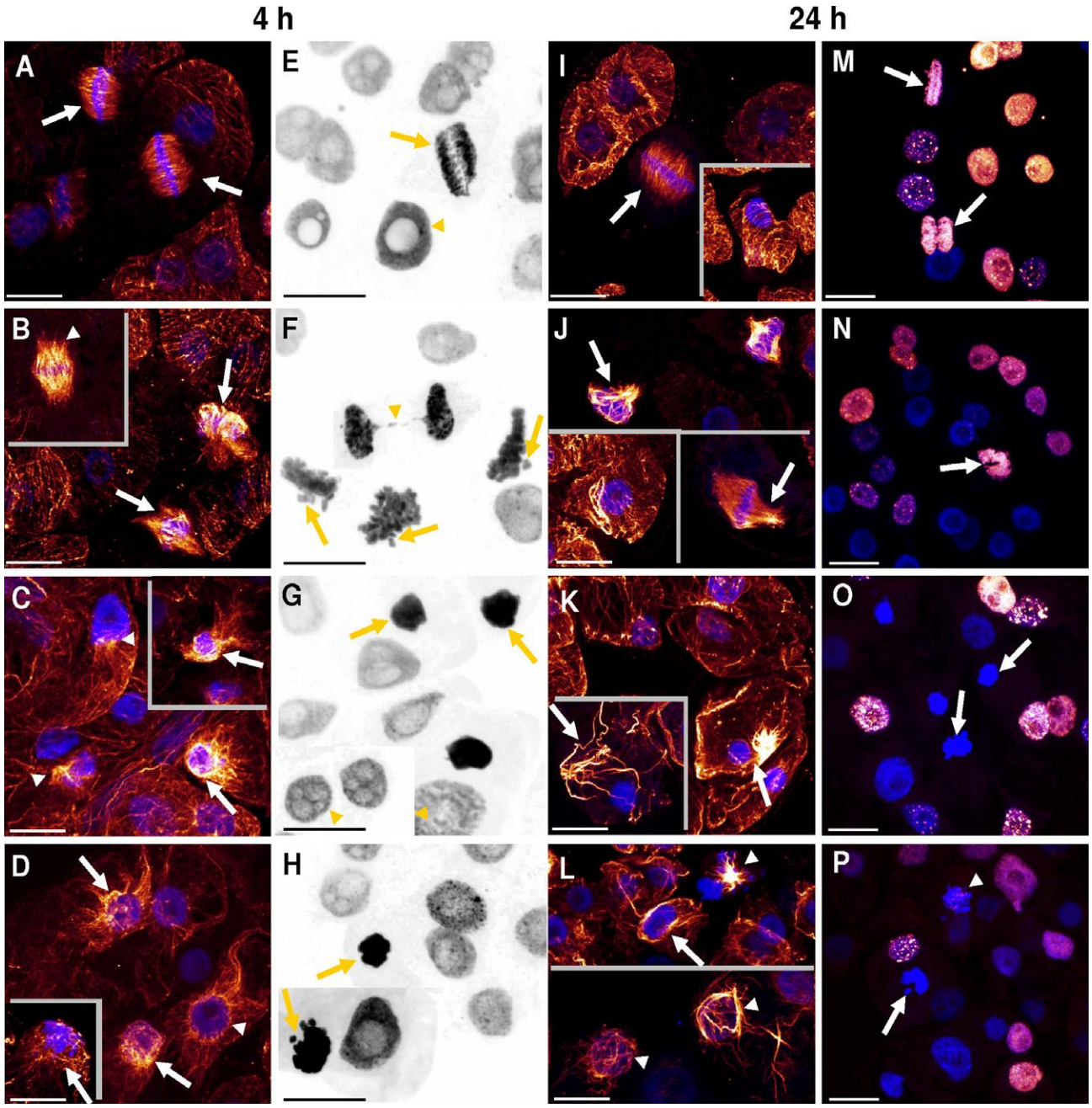

Fig. 3. Effects of endothall, cantharidin and okadaic acid on microtubule cytoskeleton and mitosis of tobacco BY-2 suspension cells. Exponentially growing BY-2 cells were treated with 10 μM compounds for 4 and 24 h and processed for fluorescence microscopic observations. (A–D) and (I–L) Immunofluorescent staining of microtubules using monoclonal antibody against β-tubulin (in red). Nuclear DNA was stained with Hoechst 33342 (in blue). Control cells (A, I) show typical mitotic phases (e.g. metaphase, arrows) and cortical microtubule patterns (I, inset). Endothall-treated cells (B), 4 h after treatment, show outspread spindle poles (inset, arrowhead) and uneven or asymmetrical mitotic spindle apparatus (arrows). Endothall-treated cells (J), 24 h after treatment, with affected spindle poles and deformed spindle apparatus (arrows). Cortical microtubules are reduced but still visible (J, inset). Cantharidin-treated cells (C), 4 h after treatment, show condensed microtubule patterns around the nucleus (C, arrows) or near by the nucleus (C, arrowheads). Cantharidin treated cells (K), 24 h after treatment, show strongly condensed and enlarged microtubule filaments often near by the nucleus, but also randomly distributed in the cell (arrows). Okadaic acid treated cells (D), 4 h after treatment, show similar changes in microtubule pattern than cantharidin. Nuclei are surrounded by condensed microtubules (D, arrows). Okadaic acid treated cells (L), 24 h after treatment, show condensed microtubule patterns in prophase or metaphase nuclei (L, arrowheads) and randomly distributed microtubules (L, arrow) in interphase cells. (E–H) and (M–P) Hoechst 33342 staining of nuclei. (M–P) Additional EdU labeling of nuclei (color coded in red) to visualize compound effects on cell proliferation. Characteristic structures of nuclei during cell cycle and mitosis are shown for each compound. Control cells (E), show distinct mitotic chromosome structures like anaphase (arrow). After 4 h of treatment, endothall-treated cells (F) show deformed chromosome structures (arrowhead), classified as prometaphase and incomplete distribution of chromosomes during mitosis (arrows). Cantharidin-treated cells (G) show strongly condensed nuclei (arrows) and relaxed nuclei structure (arrowhead). Okadaic acid (H) induces accumulation of strongly condensed nuclei (arrows) and few relaxed nuclei structures. Within 24 h, most of the control cells (M) entered or passed S-phase (red nuclei), including cells in mitotic phases. Metaphase and telophase nuclei show fluorescence which indicated EdU incorporation during S-phase (arrows). Endothall treated cells (N) show decreased S-phase transition and nuclei in mitosis with EdU incorporation (arrow). Cantharidin-treated cells (O) show few interphase nuclei with EdU incorporation, whereas strongly condensed nuclei do not show EdU mediated fluorescence (arrows). Okadaic acid-treated cells (P) also show no EdU mediated fluorescence (arrow). Prometaphase nuclei show only marginal EdU labeling (arrowhead).

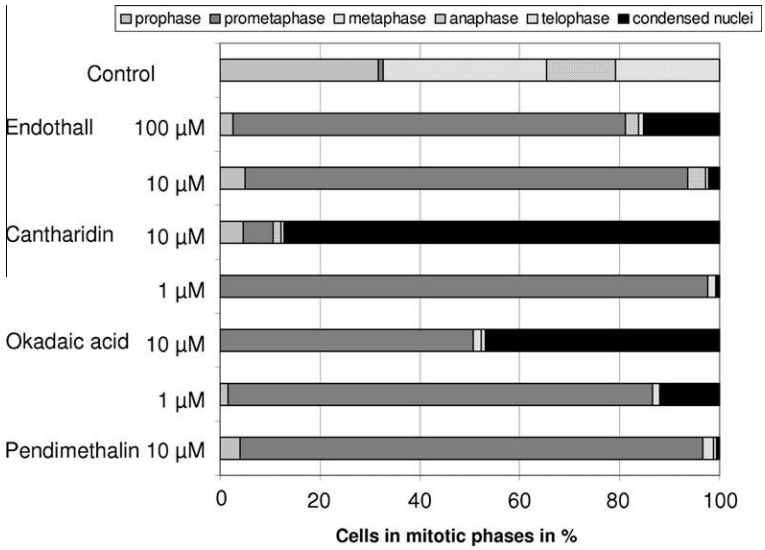

Fig. 4. Effects of endothall, cantharidin, okadaic acid and pendimethalin on the distribution of mitotic phases in tobacco BY-2 cells. Suspension cells were treated with compounds for 4 h. Hoechst 33342 stained nuclei of formalin fixed BY-2 cells were classified according to their cell cycle phase. Mitotic stages were categorized by microscopic observation of at least 500 cells per sample. Means of 4 biological replicates are shown. Cells in distinct mitotic phases were calculated as percent to total number of mitotic cells.

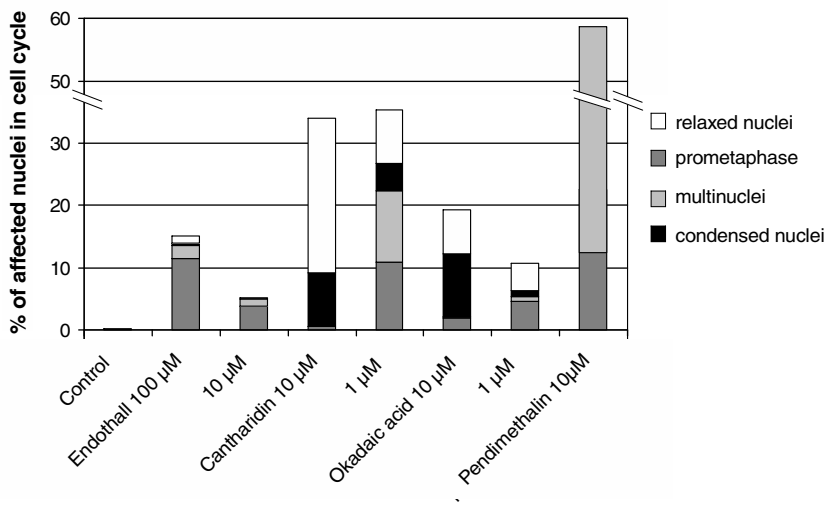

Fig. 5. Malformative effects on nucleus structure in different cell cycle phases induced by endothall, cantharidin, okadaic acid and pendimethalin in tobacco BY-2 cells. Hoechst 33342 stained nuclei of compound treated cells were classified as normal interphase, prophase, metaphase, anaphase or telophase nuclei. Malformed nuclei were classified as relaxed nuclei, prometaphase, multinuclei and strongly condensed nuclei. Relaxed nuclei were defined by their unusual Hoechst 33342 staining appearance and loosening of nucleus structure. Malformed nuclei of the distinct classes were calculated as percent to total number of affected nuclei and to total number of examined cells.

pattern of endothall and cantharidin in the bioassays together with typical plant symptoms like swelling of the meristematic root tip zone in cress seedlings showed strong similarity to inhibitors of microtubule assembly in mitosis such as pendimethalin (Fig. 1). The symptoms of tissue desiccation and necrosis which are, compared to pendimethalin, more dominant in endothall- or cantharidin-treated tissues are more typical for inhibitors which interfere with photosynthesis related processes and therefore induce reactive oxygen species, leading to cell death. These necrosis effects of endothall at high compound concentrations [4] could be based on inhibition of protein phosphatase regulated enzymes like nitrate reductase [11], sucrose phosphate synthase or hydroxymethylglutaryl-CoA reductase (reviewed by [26]). In addition, the observed slight uncoupler activity of endothall and cantharidin (Fig. 1) might contribute to membrane damage and leaf necrosis. However, further study is needed to clarify the mode of action behind the necrosis effects of endothall at high compound concentrations.

The relatively high endothall concentrations needed for induction of necrosis and the similarity of the physiological profile to mitosis inhibitors suggests that effects on cell division processes are the primary mode of action of endothall and cantharidin. Therefore, our advanced studies were focused on affected cell division processes. A direct interference of endothall in tubulin polymerization to microtubules does not appear to be the case, because endothall did not affect plant tubulin polymerization *in vitro* (Table 1). As shown in meristematic corn root tips, endothall has a strong distorting influence on the orientation of the cell division plane and microtubule spindle structures (Fig. 2). This effect was different to known microtubule assembly inhibitors such

Table 2
Changes in mitotic index (MI) and proliferation index (PI) in BY-2 tobacco suspension cells treated with endothall, cantharidin, okadaic acid and pendimethalin. Mitotic index was calculated as percent of cells in mitosis to total counted cells. Proliferation index was calculated as percent of fluorescent cells with EdU incorporation into DNA during S-phase to total counted cells.

	(μM)	4 h		24 h	
		MI	PI	MI	PI
Control		10.3 (±0.5)	24.1 (±1.4)	14.7 (±0.4)	86.0 (±5.0)
Endothall	100	12.3 (±1.1)	13.5 (±0.3)	16.4 (±1.0)	15.4 (±6.8)
	10	13.7 (±1.0)	17.1 (±3.6)	5.6 (±0.4)	47.1 (±1.6)
Cantharidin	10	14.4 (±1.0)	13.3 (±2.5)	8.5 (±0.6)	21.2 (±5.6)
	1	13.5 (±1.1)	18.8 (±2.0)	14.6 (±1.1)	17.6 (±1.0)
Okadaic acid	10	13.7 (±0.7)	14.1 (±2.9)	9.8 (±1.3)	8.0 (±3.4)
	1	14.0 (±1.7)	9.6 (±1.4)	6.1 (±0.5)	18.3 (±4.0)
Pendimethalin	10	17.9 (±1.5)	26.8 (±2.0)	22.9 (±1.2)	73.1 (±5.5)

as the dinitroaniline pendimethalin or flamprop-*m*-methyl [21,25]. Division plane orientation in corn cells has also been shown to be governed by DISCORDIA1 (DCD1) a homologue of the TONNEAU2 (TON2) protein in *Arabidopsis thaliana*, which functions as a regulatory subunit of protein phosphatases PP2As [27,28]. In accordance to microscopic observations in T-DNA inserted *A. thaliana ton1* and *ton2* mutants [28,29], most of the corn root cells undergoing mitosis were blocked by endothall in metaphase and chromosomal metaphase plates showed a diagonal orientation and were not aligned transversally as in untreated cells (Fig. 2). In addition, defective mitotic spindle microtubules oriented diagonally in the cell, similar to *ton1* and *ton2* mutant phenotypes, were observed in endothall treated plants. Studies in *ton1* and *ton2* mutants additionally revealed loss of preprophase band structures [28,29], which were also apparent in endothall-treated corn root cells (not shown). Walker et al. [30] described a relationship between TANGLED protein, which identifies the cell division plane throughout mitosis and cytokinesis, and TON2 pathway. Localization of TANGLED protein is disturbed in preprophase band defective *ton2* mutants. *tangled* mutants are affected in correct cell division plane orientation [30]. In conclusion, endothall-induced changes in microtubule cytoskeleton and cell division plane orientation resemble abnormalities observed in *Arabidopsis ton1* and *ton2* mutants [28,29]. Since endothall is an inhibitor of protein phosphatase PP2A *in vitro* [11,12], a direct effect of endothall on the functional protein complex of catalytic subunit PP2A and regulatory PP2A subunit TON2 could be expected to cause distorted microtubules and division plane orientation leading to mitotic disruption.

Further support of a causal relationship between protein phosphatase inhibition and effects on mitosis, is given by the observation of perinuclear microtubules patterns. This condensed pattern of microtubules around the nucleus was observed in *ton1* and *ton2* mutants [28,29] as well as in BY-2 tobacco suspension cells treated with endothall, cantharidin and the structurally different okadaic acid (Fig. 3). This effect was most pronounced in BY-2 cells treated with cantharidin and particularly with the more specific PP2A inhibitor okadaic acid. Mammalian PP2A responded 50 times more sensitive to okadaic acid than PP1 [31]. Endothall treatment elicited perinuclear microtubule patterns particularly at high concentration (100 μM). Treatment with 10 μM caused perinuclear microtubule patterns only occasionally. This could be due to less enzymatic inhibitor activity or PP2A sensitivity to endothall. Erdödi et al. [10] reported that, compared to PP1, mammalian PP2A responded only 3-fold and 1.8-fold more sensitive to cantharidin and endothall, respectively. This corresponds with data reported by [12] on the sensitivity of plant PP2A and PP1 to endothall.

Although the so far discussed effects of the protein phosphatase inhibitors including distorted microtubule and division plane orientation and perinuclear microtubule pattern correspond to the *ton1* and *ton2* phenotype, additional phenomena appear to be not based on TON2-pathway inhibition. These phenomena include especially the effects of the protein phosphatase inhibitors on distinct mitotic DNA phases and proliferation, which were not observed in *ton1* and *ton2* mutants. Nevertheless, induction of condensed nuclei in treated BY-2 cells appears to be also an effect based on PP2A inhibition. Snaith et al. [32] described *Drosophila* PP2A *mts* mutants with similar strongly condensed nuclei in embryos. In addition, condensed nuclei were also observed after endothall treatment of alfalfa cells [12]. However, it was difficult to evaluate in which cell cycle phase the condensed nuclei were arrested. In BY-2 cells, EdU labeling of nuclei revealed that none of the condensed nuclei contains artificial nucleotide EdU. This indicates that these nuclei have not entered S-phase with DNA replication during treatment with protein phosphatase inhibitors. It was speculated by [12] that these condensed nuclei are arrested in early prophase. This would implicate that protein phosphatase inhibitors interfere with mitosis and block S-phase entry and consequently, DNA replication. Based on our analysis of proliferation and detailed morphological evaluation of nuclei structure, it seems that the condensed nuclei are in late mitosis and are not able to undergo S-phase. This is supported by the observation of the fine structure of condensed nuclei. Whereas, chromosome like structures could be identified (Fig. 3O and H). Generally, BY-2 cells treated with endothall, cantharidin and okadaic acid showed strongly reduced proliferation activity, but EdU incorporation during DNA replication was not completely blocked. This suggests that S-phase transition from G1 is blocked, but ongoing DNA replication in S-phase cells is not or only less affected. Therefore, in addition to mitosis arrest, S-phase initiation might be an additional target site for protein phosphatase regulation.

Based on investigations in mammalian cells where PP1 activity was neutralized by an antibody, cells in mitosis where blocked at metaphase [33]. Derived from this effect, it could be speculated that the block during mitosis in BY-2 cells, characterized by condensed nuclei, could be based on PP1 inhibition by the compounds. This speculation is also supported by the observation that the strongest accumulation of condensed nuclei occurred after cantharidin treatment, which has a strong inhibitory effect on PP1 [10]. Okadaic acid was shown to possess a higher selectivity for PP2A inhibition and therefore, PP1 regulated processes should be less affected [31]. Endothall was found to be a 10-fold less potent protein phosphatase inhibitor than cantharidin *in vitro* [10,11]. This explains why endothall caused identical cell cycle phenomena to cantharidin in BY-2 cells, but, at higher compound concentration. The results suggest that, dependent on the protein phosphatase inhibitors used and their different potency and preference to PP1, PP2A or other phosphatases, slightly different phenotypes at the cytological level are induced. Additional experiments with inhibitors, such as fostriecin or tautomycetin [34,35], which act possibly more specific on the different protein phosphatases in plants, could clarify the distinct roles of the protein phosphatases in the cell cycle processes in more detail.

5. Conclusions

Supported by physiological and cytological investigations in comparison with known mitosis or protein phosphatase inhibitors,

the preferred phytotoxic mode of action of endothall appears to be based on changes in microtubule array formation and cell cycle regulation in meristematic cells, which lead to mitotic disruption, inhibition of cell division and, ultimately, to cell death. This suggests that endothall and cantharidin induced effects on cell cycle processes are mediated by protein phosphatase inhibition. Because of similarity of endothall-induced distorted microtubule array and division plane orientation, to phenomena observed in *ton1* and *ton2 Arabidopsis* mutants [28,29], we suggest that PP2A/TON2 protein phosphatase complex is an *in planta* molecular target of endothall. On the other hand, the endothall-induced phenomena of condensed nuclei, which indicate late mitosis arrest, and block of S-phase initiation in BY-2 cells, might be caused by inhibition of PP1 and/or other protein phosphatases related to PP2A.

Based on the mode of action discovery, endothall and cantharidin can be used in basic research as additional probes to unravel the function of the different types of protein phosphatases in plant cell cycle regulation.

Acknowledgments

We are grateful to Wolfgang Wernicke (University of Mainz, Germany) for kindly forwarded to us BY-2 cell cultures and valuable discussion. We also thank Günter Caspar and Manuela Wetternach for excellent technical assistance and Thomas Ehrhardt for critical reading the manuscript.

References

[1] N. Tischler, J.C. Bates, G.P. Quimba, A new group of defoliant-herbicidal chemicals, Proc. Ann. Meeting Northeastern Weed Control Conf. 4 (1951) 51–83.
[2] S.A. Senseman, Herbicide Handbook, ninth ed., Weed Sci. Soc. of Am., 2007.
[3] S.M. Wilson, A. Daniel, G.B. Wilson, Cytological and genetical effects of the defoliant endothal, J. Heredity 47 (1956) 151–155.
[4] A. Rikin, B. Rubin, Increase of cotton cotyledon resistance to the herbicide endothall by abscisic acid, Physiol. Plant. 59 (1983) 161–164.
[5] J.D. Mann, M. Pu, Inhibition of lipid synthesis by certain herbicides, Weed Sci. 16 (1968) 197–198.
[6] J.D. Mann, L.S. Jordan, B.E. Day, A survey of herbicides for their effect upon protein synthesis, Plant Physiol. 40 (1965) 840–844.
[7] D. Penner, F.M. Ashton, Influence of dichlobenil, endothall, and bromoxynil on kinin control of proteolytic activity, Weed Sci. 16 (1968) 323–326.
[8] R.-C. Tsay, F.M. Ashton, Effect of several herbicides on dipeptidase activity of squash cotyledons, Weed Sci. 19 (1971) 682–684.
[9] Y.-M. Li, J.E. Casida, Cantharidin-binding protein: identification as protein phosphatase 2A, Proc. Natl. Acad. Sci. USA 89 (1992) 11867–11870.
[10] F. Erdödi, B. Toth, K. Hirano, M. Hirano, D. J Hartshorne, P. Gergely, Endothall thioamide inhibits protein phosphatases-1 and -2A in vivo, Am. J. Physiol. 269 (1995) 1176–1184.
[11] Y.-M. Li, C. MacKintosh, J.E. Casida, Protein phosphatase 2A and its [^{3}H] cantharidin/[^{3}H]endothall thioanhydride binding site – inhibitor specifity of cantharidin and ATP analogues, Biochem. Pharmacol. 46 (1993) 1435–1443.
[12] F. Ayaydin, E. Vissi, T. Mesaros, P. Miskolczi, I. Kovacs, A. Feher, V. Dombradi, F. Erdödi, P. Gergely, D. Dudits, Inhibition of serine/threonine-specific protein phosphatases causes premature activation of cdc2MsF kinase at G2/M transition and early mitotic microtubule organisation in alfalfa, Plant J. 23 (2000) 85–96.
[13] K. Grossmann, What it takes to get a herbicide's mode of action. Physionomics, a classical approach in a new complexion, Pest Manage. Sci. 61 (2005) 423–431.
[14] S. Tresch, P. Plath, K. Grossmann, Herbicidal cyanoacrylates with antimicrotubule mechanism of action, Pest Manag. Sci. 61 (2005) 1052–1059.
[15] E.M. Linsmaier, F. Skoog, Organic growth factor requirements of tobacco tissue cultures, Physiol. Plant. 18 (1965) 100–127.
[16] S.E. Ruzin, Plant Microtechnique and Microscopy, Oxford University Press, Oxford, 1999.
[17] T. Nagata, Y. Nemoto, S. Hasezawa, Tobacco BY-2 cell line as the "HeLa" cell in the cell biology of higher plants, Int. Rev. Cytol. 132 (1992) 1–30.
[18] S. Hasezawa, T. Sano, T. Nagata, The role of microfilaments in the organization and orientation of microtubules during the cell cycle transition from M phase to G1 phase in tobacco BY-2 cells, Protoplasma 202 (1998) 105–114.
[19] A. Salic, T.J. Mitchison, A chemical method for fast and sensitive detection of DNA synthesis in vivo, Proc. Natl Acad. Sci. USA 105 (2008) 2415–2420.
[20] E. Kotogany, D. Dudits, G.V. Horvath, F. Ayaydin, A rapid and robust assay for detection of S-phase cell cycle progression in plant cells and tissues by using ethynyl deoxyuridine, Plant Methods 6:5 (2010).
[21] S. Tresch, R. Niggeweg, K. Grossmann, The herbicide flamprop-M-methyl has a new antimicrotubule mechanism of action, Pest Manag. Sci. 64 (2008) 1195–1203.
[22] D. Bonne, C. Heusele, C. Simon, D. Pantaloni, 4',6-Diamidino-2-phenylindole, a fluorescent probe for tubulin and microtubules, J. Biol. Chem. 260 (1985) 2819–2825.
[23] R.G. Anthony, P.J. Hussey, Dinitroaniline herbicide resistance and the microtubule cytoskeleton, Trends Plant Sci. 4 (1999) 112–116.
[24] S. Hasezawa, T. Nagata, Okadaic acid as a probe to analyse the cell cycle progression in plant cells, Bot. Acta 105 (1992) 63–69.
[25] J.C. Hoffman, K.C. Vaughn, Mitotic disrupter herbicides act by a single mechanism but vary in efficacy, Protoplasma 176 (1994) 16–25.
[26] R.D. Smith, J.C. Walker, Plant protein phosphatases, Annu. Rev. Plant Physiol. Plant Mol. Biol. 47 (1996) 101–125.
[27] A.J. Wright, K. Gallagher, L.G. Smith, *discordia1* and alternative *discordia1* function redundantly at the cortical division site to promote preprophase band formation and orient division planes in maize, Plant Cell 21 (2009) 234–247.
[28] C. Camilleri, J. Azimzadeh, M. Pastuglia, C. Bellini, O. Grandjean, D. Bouchez, The *Arabidopsis* TONNEAU2 gene encodes a putative novel protein phosphatase 2A regulatory subunit essential for the control of the cortical cytoskeleton, Plant Cell 14 (2002) 833–845.
[29] J. Azimzadeh, P. Nacry, A. Christodoulidou, S. Drevensek, C. Camilleri, N. Amiour, F. Parcy, M. Pastuglia, D. Bouchez, *Arabidopsis tonneau1* proteins are essential for preprophase band formation and interact with centrin, Plant Cell 20 (2008) 2146–2159.
[30] K.L. Walker, S. Müller, D. Moss, D.W. Ehrhardt, L.G. Smith, *Arabidopsis* TANGLED identifies the division plane throughout mitosis and cytokinesis, Curr. Biol. 17 (2007) 1827–1836.
[31] H. Fujiki, M. Suganuma, Tumor promotion by inhibitors of protein phosphatases 1 and 2A: the okadaic acid class of compounds, Adv. Cancer Res. 61 (1993) 143–194.
[32] H.A. Snaith, C.G. Armstrong, Y. Guo, K. Kaiser, P.T.W. Cohen, Deficiency of protein phosphatase 2A uncouples the nuclear and centrosome cycles and prevents attachment of microtubules to the kinetochore in Drosophila microtubule star (mts) embryos, J. Cell Sci. 109 (1996) 3001–3012.
[33] A. Fernandez, D.L. Brautigan, N.J.C. Lamb, Protein phosphatase type 1 in mammalian cell mitosis: chromosomal localization and involvement in mitotic exit, J. Cell Biol. 116 (1992) 1421–1430.
[34] A.H. Walsh, A.Y. Cheng, R.E. Honkanen, Fostriecin, an antitumor antibiotic with inhibitory activity against serine/threonine protein phosphatases types 1 (PP1) and 2A (PP2A), is highly selective for PP2A, FEBS Lett. 416 (1997) 230–234.
[35] S. Mitsuhashi, N. Matsuura, M. Ubukata, H. Oikawa, H. Shima, K. Kikuchi, Tautomycetin is a novel and specific inhibitor of serine/threonine protein phosphatase type 1, PP1, Biochem. Biophys. Res. Commun. 287 (2001) 328–331.